Price and Germino *Fire Ecology* (2022) 18:23
https://doi.org/10.1186/s42408-022-00147-2

Fire Ecology

Association for Fire Ecology

ORIGINAL RESEARCH

Open Access

Modeling of fire spread in sagebrush steppe using FARSITE: an approach to improving input data and simulation accuracy

Samuel "Jake" Price and Matthew J. Germino*

Abstract

Background: Model simulations of wildfire spread and assessments of their accuracy are needed for understanding and managing altered fire regimes in semiarid regions. The accuracy of wildfire spread simulations can be evaluated from post hoc comparisons of simulated and actual wildfire perimeters, but this requires information on pre-fire vegetation fuels that is typically not available. We assessed the accuracy of the Fire-Area Simulator (FARSITE) model parameterized with maps of fire behavior fuel models (FBFMs) obtained from the widely used LANDFIRE, as well as alternative means which utilized the classification of Rangeland Analysis Platform (RAP) satellite-derived vegetation cover maps to create FBFM maps. We focused on the 2015 Soda wildfire, which burned 113,000 ha of sagebrush steppe in the western USA, and then assessed the transferability of our RAP-to-FBFM selection process, which produced the most accurate reconstruction of the Soda wildfire, on the nearby 2016 Cherry Road wildfire.

Results: Parameterizing FARSITE with maps of FBFMs from LANDFIRE resulted in low levels of agreement between simulated and observed area burned, with maximum Sorensen's coefficient (SC) and Cohen's kappa (K) values of 0.38 and 0.36, respectively. In contrast, maps of FBFMs derived from unsupervised classification of RAP vegetation cover maps led to much greater simulated-to-observed burned area agreement (SC = 0.70, $K = 0.68$). The FBFM map that generated the greatest simulated-to-observed burned area agreement for the Soda wildfire was then used to crosswalk FBFMs to another nearby wildfire (2016 Cherry Road), and this FBFM selection led to high FARSITE simulated-to-observed burned area agreement (SC = 0.80, $K = 0.79$).

Conclusions: Using RAP to inform pre-fire FBFM selection increased the accuracy of FARSITE simulations compared to parameterization with the standard LANDFIRE FBFM maps, in sagebrush steppe. Additionally, the crosswalk method appeared to have regional generalizability. Flanking and backfires were the primary source of disagreements between simulated and observed fire spread in FARSITE, which are sources of error that may require modeling of lateral heterogeneity in fuels and fire processes at finer scales than used here.

Keywords: Annual grass, Fire model, Fire reconstruction, Fuel beds

*Correspondence: mgermino@usgs.gov

US Geological Survey, Forest and Rangeland Ecosystem Science Center, Boise, ID, USA

Resumen

Antecedentes: Los modelos de simulación de propagación del fuego son críticamente necesarios para el manejo y estudio de los cambiantes regímenes de fuego de regiones semiáridas, especialmente para el ciclo expansivo de fuego-cheatgrass (*Bromus tectorum*)--fuego en la vasta región de la estepa de artemisia (sagebrush steppe) de América del Norte. Comparando la propagación simulada del fuego con los patrones reales de propagación, los manejadores de recursos e investigadores pueden calibrar la confiabilidad y exactitud de la propagación simulada y sus entradas de datos de combustibles, aunque esto requiere de datos previos de vegetación y otra información que está típicamente disponible sólo en datos modelados, especialmente para grandes incendios. Determinamos la exactitud del modelo de propagación FARSITE (*Fire-Area Simulator spread model*) usando opciones alternativas de entrada de datos para el incendio de Soda de 2015 (*Soda Fire*) que quemó 113.000 ha de la estepa de artemisia por 6 días en Oregon y Idaho, EEUU, y luego determinaos la transferibilidad del modelo a otro incendio.

Resultados: La parametrización de FARSITE con los datos de combustible del LANDFIRE resultaron en bajos niveles de ajuste entre el área quemada simulada y observada, con valores máximos del Coeficiente de Sorensen (SC) y del de Cohen Kappa (K) de 0,38 y 0,36, respectivamente. Para mejorar el ajuste entre las áreas quemadas (real y simulada), probamos una alternativa de entrada de datos usando la clasificación no supervisada de máxima probabilidad derivada de mapas de vegetación basados en datos satelitales de la plataforma *Rangeland Analysis Platform* (RAP), y determinamos cómo diferentes opciones para ajustar las clasificaciones de cobertura de suelo resultantes a los modelos standard de comportamiento de combustibles (FBFMs), afectaban la exactitud del FARSITE. El uso del RAP para informar la selección del FBFMs, llevó a un mejor ajuste de los resultados entre las simulaciones del FIRESITE y el perímetro real del fuego (SC=0,70 y K=0,68). La parametrización de la cobertura de suelo basada en RAP de los modelos FBFMs desarrollados para el incendio de Soda fue usado para las simulaciones del incendio de la Ruta Cherry en 2016 (*Cherry Road fire*) y resultaron en una alta exactitud (SC= 0,80 y K=0.79).

Conclusiones: El uso de la Plataforma RAP para informar sobre la selección de FBFM incrementó la exactitud de las simulaciones del FARSITE en relación a los perímetros quemados comparado con el standard de los mapas previos usados corrientemente de FBDMs basados en LANDFIRE, para la estepa de artemisia. El método parece tener una generalización regional, lo que indica que el proceso total de selección del FBFM realizado aquí puede no ser necesario para cada incendio individual. Los fuegos de flanco y en retroceso fueron la fuente primaria de divergencias en la propagación entre los fuegos simulados y observados en FARSITE, las cuales fueron fuentes de error que podrían requerir el modelado de la heterogeneidad lateral en los combustibles y procesos de fuego a escalas más finas que las usadas en este trabajo.

Introduction

Model simulations of wildfire behavior and spread then provide critical information for effective fuels and wildfire management, including in the semiarid sagebrush steppe of the western USA where large wildfires are becoming increasingly common and impactful, owing to the invasive grass-fire cycle (Balch et al. 2013; Dennison et al. 2014; Germino et al. 2016). Fire spread and/or behavior can be predicted in wildlands using models such as Fire Area Simulator (FARSITE) and Minimum Travel Time (MTT; Finney 1998, 2002), such as fire-suppression operations with the US Wildland Fire Decision Support System (WFDSS; Noonan-Wright et al. 2011) or to plan fuel treatments in sagebrush steppe. However, there are few validations of MTT and FARSITE or their fuel-input options in sagebrush steppe or other patchy, low-statured plant communities of semiarid areas. The primary means for assessing the accuracy of these fire-model estimates is to compare simulated to observed wildfire behavior and/or perimeters, but this requires pre-fire vegetation and fuel information that is typically not available, especially in sagebrush steppe where prescribed fires are scarce (Stratton 2009; Alexander and Cruz 2013). Our objective was to evaluate available and alternative means for post hoc mapping of fuels to parameterize MTT and FARSITE simulations (Finney 2002, 2006) for reconstructing a historic megafire in sagebrush steppe.

MTT and FARSITE are based on Rothermel's (1972) surface fire spread equation, with the former able to simulate many possible ignition points for assessing generalized fire risks and the latter designed for evaluating single ignitions. MTT simulates fire spread and behavior by computing the fastest straight-line fire growth between pixel corners under a single, unchanging set of weather and fuel moisture conditions (Finney 2002). MTT requires less computation time, which facilitates iterative simulations at the tradeoff of being less suited to longer burn durations (e.g., Stratton 2009). FARSITE uses Huygens' principle to simulate wildfire spread via expanding, ellipsoidal "wave" fronts propagated from independent points that merge into multiple flaming fronts (Anderson et al. 1982; Richards 1995). Weather and fuel moisture change over space and time as fire progresses in FARSITE, requiring greater computation time, but making it more suitable for simulating longer fire periods. Fire-perimeter growth in MTT and FARSITE are nearly identical under static weather and fuel moisture conditions (Finney 2002). One limitation of these models is their assumptions that fuels are continuous and homogenous within pixels of analysis, and that there are no fire-atmospheric interactions. However, fuel configurations in sagebrush-steppe and other arid and semi-arid environments have microscale heterogeneity resulting from gaps between shrub crowns and large bare-soil interspaces that likely affect fire movement.

MTT and FARSITE require fuel-bed inputs such as fuel loading, bulk density, particle size, heat content, and moisture of extinction, all of which are parameterized in fire behavior fuel models (FBFMs) that have been developed for dominant vegetation types. The utility and reliability of fire spread models hinge strongly on the selection of FBFM(s) to represent the fuels of subject landscapes. Two libraries of FBFMs are available to parameterize Rothermel's (1972) surface fire spread equation: (1) 13 FBFMs defined by Albini (1976) and described by Anderson (1982) which are designed for the most severe fire conditions when all fuels are fully cured and (2) the 40 FBFMs defined by Scott and Burgan (2005) that expanded to more conditions in time and space, i.e., fire risks any time of year. Maps for both the Anderson 13 and Scott and Burgan 40 standard FBFMs are readily available for the entire USA from LANDFIRE (https://landfire.gov) and are often used to parameterize the spatial layout of fuels in MTT and FARSITE.

We first evaluated the accuracy of FARSITE simulations parameterized with readily available maps of FBFMs from LANDFIRE for the 2015 Soda wildfire that occurred in sagebrush steppe of the western US. Next, to determine if simulation accuracy could be improved with alternative selections of FBFMs, we selected FBFMs by using unsupervised maximum likelihood classification (ArcMap version 10.7, ESRI, Redlands, CA) of satellite-derived vegetation cover maps of the pre-fire vegetation from the USDA Rangeland Analysis Platform (RAP, Jones et al. 2018; Allred et al. 2021). We asked which spatial arrangement of FBFMs led to the best FARSITE simulation in terms of simulated-to-observed burned area agreement, and (1) identified what aspects of the simulation contributed to differences in simulated compared to observed fire perimeters and then (2) asked how well the best-performing FBFM parameterization for simulating the Soda fire performed on another nearby burned area, the Cherry Road fire, which burned through similar terrain and vegetation in 2016 (Fig. 5).

Methods

Study area and context

The Soda wildfire burned approximately 113,000 ha of native shrubs and perennial bunchgrasses, and (or) invasive annual grasses on a variety of landforms encompassing a wide range in elevation (708–2053 m), mean-annual precipitation (230–550 mm/year), and mean-annual air temperature (6.8–10.8 °C; 30-year PRISM data, 800 m pixels, Fig. 1). The entire area was grazed by livestock prior to the wildfire, with stocking rates varying from about 2 to 4 ha per animal unit month among pastures with primarily spring and summer use. Wild horses were also present on the landscape (approximately 300 horses). Grazing or browsing wildlife included primarily mule deer (*Odocoileus hemionus*) and pronghorn antelope (*Antilocapra americana*), Greater sage-grouse (*Centrocercus urophasianus*), and a range of small mammals (e.g., lagomorphs, ground squirrels). Considerable post-fire restoration/rehabilitation treatments were conducted on the Soda burned area (Germino et al. 2022) and were followed by the installation of a network of linear fuel breaks to help protect the landscape and investments from reburning (Soda Fire Fuel Breaks Environmental Impact Statement, 2017). Thus, there is keen interest in understanding how simulated fire risks relate to vegetation recovery and vegetation management options for this particular landscape, which first requires assessing how well fire can be modeled across the landscape.

Case study

The Soda wildfire ignited eight miles northeast of Jordan Valley, Oregon, and burned approximately 110,000 ha from August 10 through 15 (Fig. 1). The fire was officially contained on August 23 burning a total of 113,000 ha, within months following the landmark Department of Interior Secretarial Order #3336 on Rangeland Fire Suppression and Restoration (Jewell, 2015) that prioritized rapid suppression to reduce losses of sagebrush steppe habitat. Weather conditions preceding the fire were hotter and drier than normal (described in the "Input data for fire simulations" section) and resulted in uncharacteristically low live fuel moisture. Fuels across the area primarily consisted of shrubs with considerable amounts of dead wood and a mix of perennial and annual grasses. The ignition occurred in a grass and shrub community with mean wind speeds arriving from the south at 16–32 km/h but gusting to 45 and 56 km/h, which

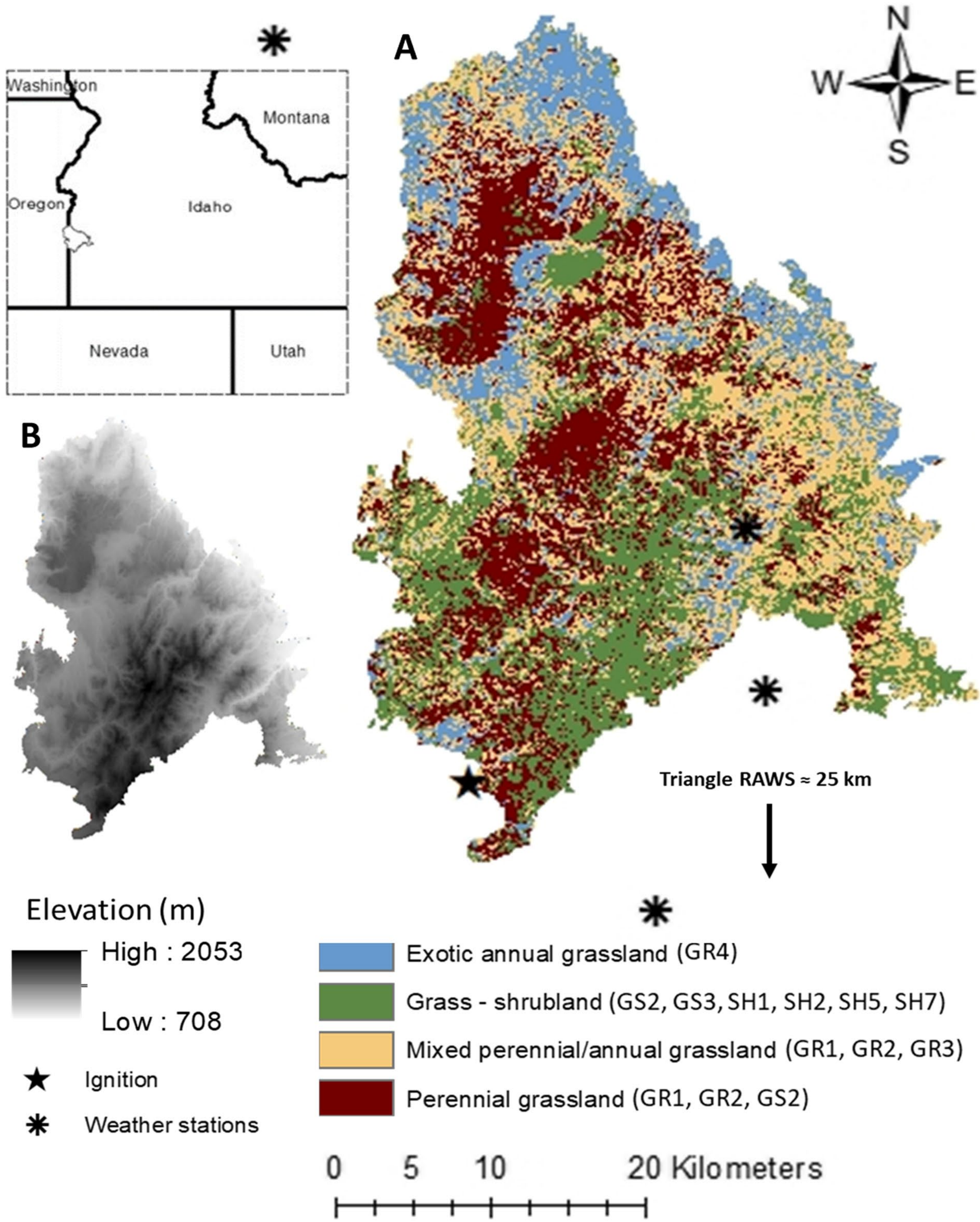

Fig. 1 Land-cover types and corresponding arrays of possible fire behavior fuel models for fire-spread simulations (**A**, from unsupervised classification) and elevation (**B**) for the study area, as well as ignition point, and weather station locations used for the 2015 Soda wildfire simulations. The inset map shows the location of the Soda wildfire along the Idaho and Oregon border, USA. The scale bar aligns to the land-cover type map

were recorded at the Owhyee Ridge and Triangle Remote Automatic Weather Stations (RAWS) located approximately 5 km north and 25 km south of the burn area, respectively (Fig. 1). High sustained winds and continuous flashy fuels contributed to rapid rates of fire spread up to 150 m/min. Observed flame lengths were 2.5–3 m in grass and 6–9 m in shrubs (Soda Fire Fuel Breaks Environmental Impact Statement, 2017).

Land-cover type classifications and fuel model assignments

An overview of the following workflows can be found in Supplementary Figure 1. Canopy and fuel maps for use in MTT and FARSITE are often parameterized using LANDFIRE datasets including the Scott and Burgan 40 or Anderson 13 FBFMs (https://LandFire.gov). FARSITE simulations of the Soda wildfire using LANDFIRE fuel and canopy maps as input (LF 2014 – LF 1.4.0), however, produced wildfire spread with poor agreement compared to the observed burn perimeter (Fig. 2). Inspection of LANDFIREs inputs revealed potential inaccuracies in the canopy and fuels layers within the Soda wildfire boundary. For example, LANDFIRE had mapped ~6% of the study area as either having an overstory (i.e., trees) or timber-type fuel models with high loads of coarse fuels located where, to our knowledge, none had existed. Moreover, 86% and 96% of the study area mapped by LANDFIRE's FBFM 40 and FBFM 13 fuel datasets, respectively, were comprised of only three FBFMs (Fig. 2) of which ~44% were mapped as either FBFM 1 (short grass; Anderson 1982) or FBFM GR2 (low load, dry climate grass; Scott and Burgan 2005; Fig. 2).

As an alternative way to establish fuels across the burned area, we created a coarse land-cover type map by starting with readily available data from the USDA Rangeland Analysis Platform (RAP), which combines field monitoring plots from the US Bureau of Land Management (BLM) Assessment, Inventory and Monitoring program and the NRCS National Resources Inventory, as well as historic Landsat satellite records to generate yearly predictions of continuous cover (from 0 to 100%) for trees, shrubs, perennial grasses, annual herbaceous cover, and bare soil (Jones et al. 2018; Allred et al. 2021). Though extensive post-fire monitoring data were available for the Soda Fire (e.g., over 2000 plots/year from 2016 to 2020; Germino et al. 2018, 2022; Davidson et al. 2019; Applestein and Germino 2021), pre-fire vegetation and fuel data were scarce, and thus, modeled data (i.e., RAP) was relied upon for retrospective fire simulation modeling. This extensive post-fire monitoring data, however, allowed us to assess the accuracy of RAP data across our subject landscape. For example, mean absolute error in agreement between RAP remotely sensed vegetation cover and USGS field monitoring data were ±7% for annual herbaceous cover measured in 2020 (Allred et al. 2021; Applestein and Germino 2022). Unsupervised maximum likelihood classification of RAP 2014 vegetation cover maps was used to classify the pre-Soda landscape into land-cover types. Our goal when classifying the landscape into land-cover types was to optimize the total number of classifications so that clear distinctions between dominant vegetation types could be discerned with confidence. Ultimately, four land-cover types were determined and one of each assigned to a pixel: grass-shrubland, perennial grassland, mixed perennial and annual grassland, and exotic annual grassland (Table 1; Fig. 1).

Scott and Burgan's 40 FBFMs (Scott and Burgan 2005) represent a wide range of vegetation types and ecosystems of which only a limited number (10 total) were considered by us to be appropriate for our study area (Table 1). Relevant FBFMs from the Scott and Burgan 40 set (Scott and Burgan 2005) were assigned to each pixel across the Soda landscape based on the dominant vegetation expected to be the primary carrier of fire for each land-cover type, such as assigning grassland FBFMs to pixels mapped as grassland land-cover types (Fig. 1). Given multiple appropriate FBFMs possible for each land-cover type, 14 unique FBFM combinations resulted (Table 2). Grass-dominated standard fuel models included GR1, GR2, GR3, and GR4, which are defined as short sparse dry climate grass, low load dry climate grass, low load very coarse humid climate grass, and moderate load dry climate grass, respectively. Mixed grass and shrub standard fuel models included GS1, GS2, and GS3, which are defined as low load dry climate grass-shrub, moderate load dry climate grass-shrub, and moderate load humid climate grass-shrub, respectively. Shrub-dominated fuel models included SH1, SH2, and SH5, which are defined as low load dry climate shrub, moderate load dry climate shrub, and high load dry climate shrub, respectively. Non-burnable fuel beds were assigned to main roads, agriculture, and water bodies.

Input data for fire simulations

MTT and FARSITE require similar geospatial inputs to simulate wildfire spread, including topography, weather, FBFMs, fuel moisture, and canopy characteristics. These data layers were assembled into a landscape grid file at 30-m resolution using ArcFuels 10 (v 1.2.09) in ArcMap (v 10.7). Topography layers including elevation, slope, and aspect were obtained from LANDFIRE. As previously described, the surface fuel layers were either LANDFIRE FBFM maps (Anderson 13 or Scott and

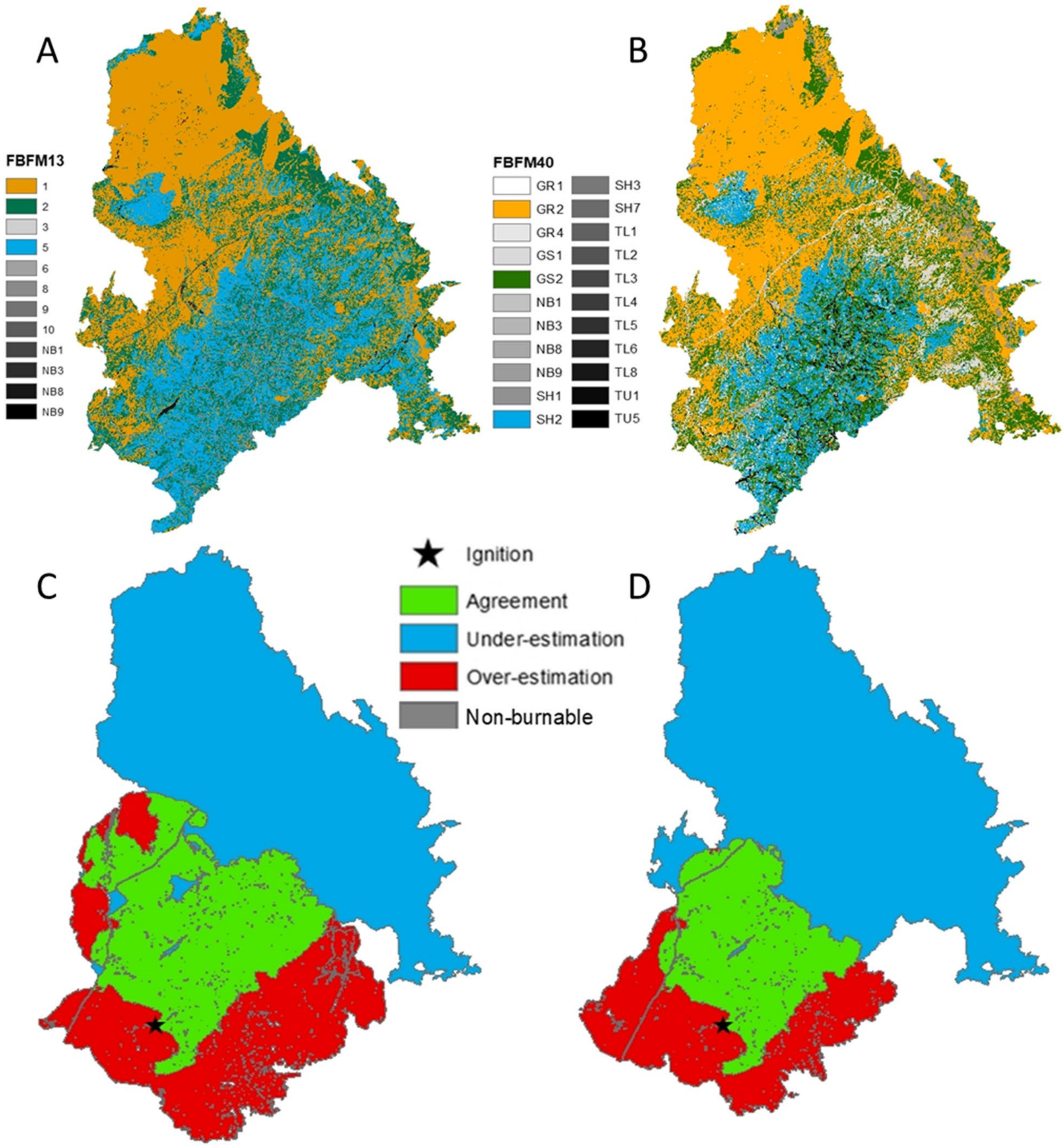

Fig. 2 Maps showing **A** Anderson's 13 fire behavior fuel models (FBFMs) mapped by LANDFIRE, **B** Scott and Burgan's 40 FBFMs mapped by LANDFIRE, **C** agreement between FARSITE simulated fire spread and the observed area burned in the 2015 Soda fire using Anderson's 13 FBFMs as input (mapped in panel **A**), and **D** agreement between FARSITE simulated fire spread and the observed burned area in the 2015 Soda fire using Scott and Burgan's 40 FBFMs as input (mapped in panel **B**). Dominant FBFMs for the study area, as mapped by LANDFIRE's Anderson's 13 FBFMs and Scott and Burgan's 40 FBFMs, accounted for 96% and 86% of the burned area, respectively, and are colored orange, blue, and green in panels **A** and **B**. Other mapped FBFMs are shown in gray scale and account for the remainder of the landscape. The sum of the blue- and green-colored polygons in panels **C** and **D** is the actual observed burn area, and the sum of green and red polygons is the area burned in FARSITE simulations

Table 1 Mean cover plus/minus standard deviation of plant functional groups that comprised the four dominant land-cover types prevailing before the 2015 Soda wildfire, and the alignment of each cover type to the most relevant fire-behavior fuel models from Scott and Burgan's 40 (2005). The land-cover classes were established using unsupervised maximum likelihood classification (ArcMap) of vegetation cover maps (USDA Rangeland Analysis Platform). See Table 2 for accuracy of different blends of the candidate fuel models

Land-cover type	Shrub cover (%)	Perennial Grass cover (%)	Annual Herbaceous cover (%)	Bare Soil cover (%)	Candidate fuel models
Grass - shrubland	31 ± 10.6	38 ± 7.8	18 ± 8.5	14 ± 6.7	GS2, GS3, SH1, SH2, SH5, SH7
Perennial grassland	15 ± 3.5	57 ± 7.5	19 ± 7.6	9 ± 3.1	GR1, GR2, GS2
Mixed perennial/annual grassland	14 ± 5.6	36 ± 6.6	39 ± 9.3	11 ± 3.8	GR1, GR2, GR3
Exotic annual grassland	8 ± 3.4	24 ± 5.6	63 ± 9.6	6 ± 2.8	GR4

Table 2 Statistical evaluation of MTT and FARSITE simulations. MTT simulations were compared to the Soda Fire perimeter as of 8/11/2015, and FARSITE simulations were compared to the much larger Soda fire perimeter on 8/15/2015. FARSITE simulations were also compared to the Cherry Road fire perimeter as of 8/22/2016 (CR1, CR2). Table 1 and Figs. 1, 2, and 3 relate FBFMs to actual land-cover types. The fuel models listed for each simulation, in order from left to right, correspond to shrubland (SH) or grass-shrubland (GS) on the left, followed by perennial grassland or mixed perennial-annual grassland (GR) and annual grassland on the right

Model	Simulation #	Fuel model combination	SC[a]	*K*[b]	*a*[c] (ha)	*b*[d] (ha)	*c*[e] *(ha)*
FARSITE	LANDFIRE-40[f]	Scott and Burgan 40	0.32	0.30	26,244	23,572	86,811
	LANDFIRE-13[g]	Anderson 13	0.34	0.32	31,958	40,459	81,097
MTT	1	(GS3, GR1, GR2, GR4)	0.59	0.58	20,139	16,002	11,511
	2	(GS2, GR1, GR2, GR4)	0.50	0.48	14,665	12,691	16,985
	3	(SH1, GR1, GR2, GR4)	0.38	0.36	9840	10,008	21,811
	4	(SH2, GR1, GR2, GR4)	0.38	0.35	9701	10,041	21,949
	5	(SH5, GR1, GR2, GR4)	0.59	0.58	27,645	33,834	4005
	6	(GS3, GR2, GR1, GR4)	0.63	0.61	21,990	16,244	9661
	7	(GS2, GR2, GR1, GR4)	0.57	0.55	18,029	13,151	13,622
	8	(SH1, GR2, GR1, GR4)	0.50	0.48	14,152	11,023	17,498
	9	(SH2, GR2, GR1, GR4)	0.50	0.48	14,090	10,891	17,561
	10	(SH5, GR2, GR1, GR4)	0.60	0.59	28,275	33,811	3376
	11	(SH5, GS2, GR2, GR4)	0.60	0.58	28,516	34,846	3109
	12	(GS3, GS2, GR2, GR4)	0.62	0.60	21,504	16,543	10,121
	13	(SH7, GS2, GR2, GR4)	0.64	0.62	25,194	22,220	6431
	14	(SH5, GS2, GR3, GR4)	0.62	0.60	28,300	31,505	3351
FARSITE	6	(GS3, GR2, GR1, GR4)	0.63	0.61	74,306	51,230	35,911
	10	(SH5, GR2, GR1, GR4)	0.68	0.66	92,222	69,850	17,994
	11	(SH5, GS2, GR2, GR4)	0.70	0.68	106,464	86,017	6592
	12	(GS3, GS2, GR2, GR4)	0.64	0.62	77,622	55,594	32,594
	13	(SH7, GS2, GR2, GR4)	0.67	0.66	74,254	35,782	35,962
	14	(SH5, GS2, GR3, GR4)	0.54	0.52	48,876	19,312	64,180
	CR1[h]	(GS2, GR2, GR4)	0.77	0.76	10,131	3452	2509
	CR2[h]	(GS2, GR3, GR4)	0.8	0.79	12,621	6439	19

[a] Sørensen's coefficient value

[b] Cohen's kappa coefficient value

[c] Burned area agreement

[d] Model overestimation

[e] Model underestimation

[f] LANDFIRE's Scott and Burgan 40 fuels' dataset

[g] LANDFIRE's Anderson 13 fuels' dataset

[h] Cherry Road wildfire simulations

Burgan 40) or our alternative FBFM maps derived from remotely sensed vegetation cover data. Canopy layers from LANDFIRE included canopy cover, height, bulk density, and base height. In the alternative FBFM maps, these variables were altered to reflect the RAP remotely sensed tree cover estimates, i.e., LANDFIRE's canopy layers were manually reduced to 0 where RAP estimated 0% tree cover.

Weather data for simulations were obtained from two RAWS stations and three US Agricultural Research Service (ARS) weather stations that span the Reynolds Creek Watershed in and outside the southeast portion of the burn area (REY012, REY076, REY124; Fig. 1). WindNinja software (v 3.6.0) was used to generate wind direction and speed vectors using these five weather stations at hourly time steps with 200-m spatial resolution.

The Soda wildfire occurred in mid-August, which tends to be the hottest and driest time of the year for the region. For August over a 30-year period, mean daily air temperature was 21°C with maxima of ~43 °C and precipitation is 8.4mm with zero precipitation in many years (PRISM, 800 m pixels). In August 2015, the mean daily air temperature was 22°C and the total precipitation was 2 mm. The National Fuel Moisture Database had recorded fuel moisture values for Wyoming Big Sagebrush in the region from August 2015 to be 60–70% (https://www.wfas.net). A prolonged drought had also been affecting the region since 2012; however, 2014 and 2015 were among the driest years in the last few decades (NOAA NIDIS, Owyhee County, Idaho; https://www.drought.gov). For the reasons outlined above, initial fuel moisture for 1 h, 10 h, 100 h, live herb, and live wood classes, for all FBFMs, were set at 3%, 4%, 5%, 30%, and 60% respectively. All dead fuels underwent a 12-h "conditioning period" in MTT and FARSITE simulations, prior to ignition. MTT and FARSITE's "conditioning period" adjusts dead fuel moisture values to account for local variation in site, such as elevation, slope/aspect, and canopy cover, and environmental factors such as air temperature, humidity, and rainfall.

A buffer around the study area was included in all MTT and FARSITE simulations, parameterized with geospatial data from the LANDFIRE Scott and Burgan 40 fuels' dataset. The purpose of this buffer around the study area was to not constrain fire spread simulations within the burn perimeter. The buffer was 5× greater in size than the Soda wildfire scar. Geospatial data from LANDFIRE used for this buffer was not altered in any way for this study.

Wildfire simulations

All fire spread simulations used 30-m pixel resolutions and burn periods were contiguous in time because nighttime lulls in fire spread were not observed or recorded. In MTT and FARSITE, "surface fires" are those fires which lack a canopy (i.e., where trees are not present) and do not produce spotting in simulations. Approximately 97% of the Soda fire simulation would then fall under this "surface fire" mode since 3% of the Soda fire was mapped to have a tree canopy. Preliminary simulations with > 0 spot probability produced rapid fire spread to the east on day two of the fire, but the Soda Fire actually spread rapidly northward, covering ~ 30 km over a 25-h burn period. Additionally, simulations using LANDFIREs default fuel and canopy inputs with >0 spot probability did not significantly improve fire spread estimates (not shown here). For these reasons spot probability was set to 0, i.e., there was no chance that spotting would contribute to fire growth. Details concerning suppression activities during the fire could not be determined for certain; however, the observed fire behavior reported describes a wildfire that was largely out of control, and so suppression was not considered in any simulations.

As stated above, FARSITE simulations were first parameterized using LANDFIRE's unaltered canopy layers and fuels inputs from the Scott and Burgan 40 and Anderson 13 pre-mapped FBFMs (Scott and Burgan 2005; Anderson 1982; Fig. 2). The low levels of agreement produced by simulations parametrized with LANDFIRE's default inputs prompted our assessment of alternative fuel mapping methods (Table 2; Fig. 2). Due to the long computation times related to FARSITE runs, the size and duration of the Soda wildfire, and the number of standard FBFM combinations that were to be tested (14 total), model calibration was first conducted in MTT to reduce the number of simulations needed to run in FARSITE to identify the optimum FBFM layout for the study area. MTT simulations used different combinations of standard FBFMs (14 total) assigned to land-cover types which we defined as grass-shrubland, perennial grassland, mixed perennial and annual grassland, and exotic annual grassland, affected during day two of the Soda wildfire (8/10/2015 @ 1900 to 8/11/2015 @ 2000; Table 2). On day two of the Soda wildfire, the fire expanded 31,000 ha over 25 h. By the end of the day two burn period, the fire front was approximately 30 km north of where it began. Weather in MTT is static, so we chose to parameterize the model using the weather from day two that had strong southerly winds (1200–1300 on 8/11/2015).

FARSITE simulations focused on the period of 8/10/2015 to 8/15/2015 when the Soda wildfire actively grew to a size of 110,000 ha. FARSITE was parametrized using combinations of standard FBFMs (Scott and Burgan 2005) which provided the highest simulated-to-observed burned area agreement in MTT based on the best reproductions of the fire perimeter at the end of the second day (6 total; Table 2). Hourly weather inputs from WindNinja were used for wind speed and direction in FARSITE simulations. Simulated fire perimeters, rate of spread (ROS), flame length (FML), and fire line intensity (FLI) were exported for each FARSITE run and analyzed in ArcMap.

We tested the local transferability of our method of assigning FBFMs derived from the satellite-based models of pre-fire vegetation to the nearby Cherry Road fire. The Cherry Road fire ignited on the afternoon of 8/21/2016 in a remote area of the Owyhee mountains, northwest of the Soda fire, and burned 12,640 ha by mid-morning on 8/22/2016 under moderate winds (avg: 16 km/h, gusts: 40 km/h), and an additional ~1360 ha over the following three days. Our FARSITE simulation focused on only the first 21 h of active burning (8/21/2016 @ 1300 -> 8/22/2016 @ 1000). Similar to our Soda Fire analysis, we identified the spatial arrangement of pre-fire land-cover types on the Cherry Road fire using the 2015 RAP dataset, which revealed three land-cover types. Likely due to the Cherry Road wildfires close proximity to the Soda wildfire and similar vegetation, land-cover types produced for both were similar (Tables 1 and 4). FBFMs assigned to land-cover types from the best performing simulation of the Soda wildfire were then used to cross-walk FBFMs to similar land-cover types for the Cherry Road wildfire (Fig. 3).

Statistical analysis

Sorensen's coefficient (SC) and Cohen's kappa (K) were used as measures of simulated-to-observed burned area agreement. SC is used as an indicator of exclusive agreement and does not account for "chance" agreement. SC was calculated as follows:

$$\mathrm{SC} = \frac{2a}{2a + b + c}$$

where a is the number of cells coded as burned in both observed and simulated data (burned area agreement), b is the number of cells coded as burned in the simulation and unburned in the observation (modeling overestimation), and c is the number of cells coded as unburned in the simulation and burned in the observation (modeling underestimation; Jhardi and Salis 2015). K assesses the agreement with adjustments that account for "chance." K was calculated as follows:

$$K = \frac{(Po - Pc)}{1 - Pc}$$

$$Po = \frac{a + d}{n}$$

$$Pc = \frac{(f1 \times g1/n) + (f2 \times g2/n)}{n}$$

where Po is agreement and Pc is agreement by chance (Filippi et al. 2014). Other variables included are as follows: a is the burned area agreement, b is model over-estimation, c is model under-estimation, d is the simulation domain, $f1$ is the sum of a and b, $f2$ is the sum of c and d, $g1$ is the sum of a and c, $g2$ is the sum of b and d, and n is the sum of $g1$ and $g2$. Both K and SC values range from 0 to 1, with values close to 1 indicating high agreement. The zonal statistics tool in ArcMap was used to analyze and summarize fire behavior data (ROS, FML, FLI).

Results

Fire simulation accuracy

FARSITE simulations using LANDFIRE's pre-mapped fuels (Anderson 13 and Scott & Burgan 40) and canopy layers as inputs resulted in SC and K values ranging from 0.31 to 0.38 and 0.29 to 0.36, respectively (agreement compared to actual fire perimeters) with slightly greater accuracy for simulations using Anderson's 13 pre-mapped FBFMs (Table 2). Simulations based on LANDFIRE's Scott and Burgan 40 and Anderson 13 pre-mapped FBFMs predicted 48,000 and 71,000 ha of total fire growth over the duration of the simulation (8/10/2015–8/15/2015) with only 25,000 and 35,000 ha burning in agreement with the observed perimeter (respectively; Fig. 2). The erroneous presence of tree cover in the LANDFIRE data input did not appear to contribute to the inaccuracy in fire spread, as additional simulations with spotting probability ranging from 0 to 100% had minimal effect on the area burned, and so tree cover was not further addressed in the assessment of LANDFIRE data inputs.

The FBFM with the highest rate of spread in FARSITE simulations using LANDFIRE's default Scott and Burgan 40 fuels datasets was GR4, which covered < 5% of the total area simulated to have burned in FARSITE (Fig. 2), though, notably, the simulated fire did not reach the large expanses of exotic annual grasslands to the northeast which did burn in reality. Another FBFM which can have high rates of spread is GS2 and covered ~30% of the area simulated to have burned, but where it was located within the LANDFIRE fuels map did not contribute to rapid fire spread in the simulation.

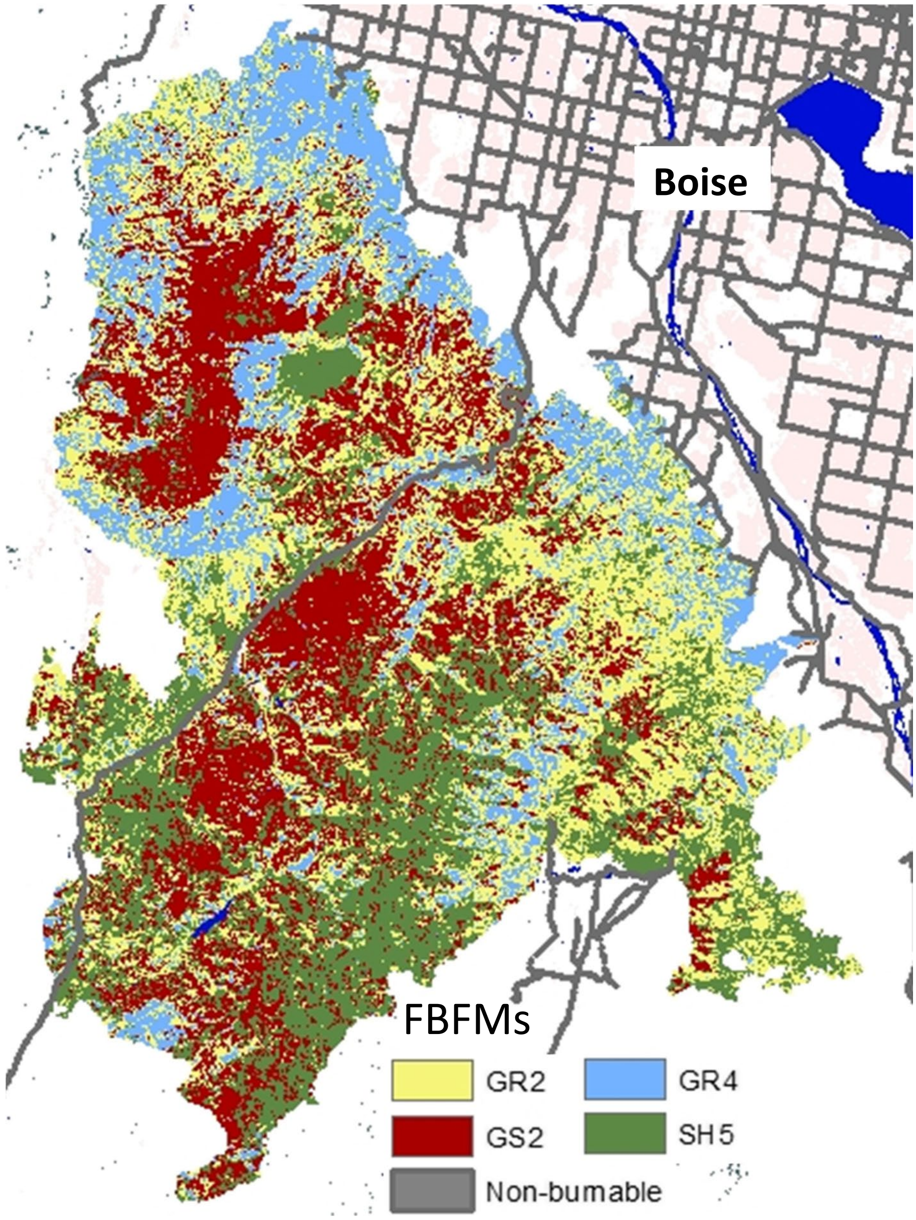

Fig. 3 The spatial layout of standard fire behavior fuel models (FBFMs) across the Soda burn scar which resulted in the highest agreement for FARSITE runs (combination #11). In this combination, SH5 was assigned to areas mapped as "grass – shrubland," GS2 to "perennial grassland," GR2 to "mixed perennial/annual grassland," and GR4 to "exotic annual grassland"

The FBFM with the highest rate of spread in the FARSITE simulation using LANDFIRE's Anderson 13 pre-mapped FBFMs was #1 (short grass), which covered ~44% of the simulated area burned (Fig. 2, FBFM #1 is orange). However, in both fuels datasets, ~75% or more of the landscape was comprised of other FBFMs that had lower rates of fire spread.

Agreement between MTT simulations and the observed burn perimeter on day two of the Soda fire ranged from 0.38 to 0.64 for SC and 0.35 to 0.62 for *K* (Table 2). MTT trials with the highest agreement (#6, 10–14), were tested further in FARSITE. SC and *K* coefficients for top-performing MTT trials were improved in FARSITE (0.54–0.7 and 0.52–0.68), respectively (Table 2). Standard FBFM GR4 was included in all fuel landscapes (representing exotic annual grassland), and so variability in accuracy resulted from which models represented the other three land-cover types (grass-shrubland, perennial grassland, mixed perennial and annual grassland). Only fuel models SH1 and SH2 did not contribute to any of the most accurate FBFM combinations. Of the 7 FBFMs that contributed to the 6 most-accurate combinations of

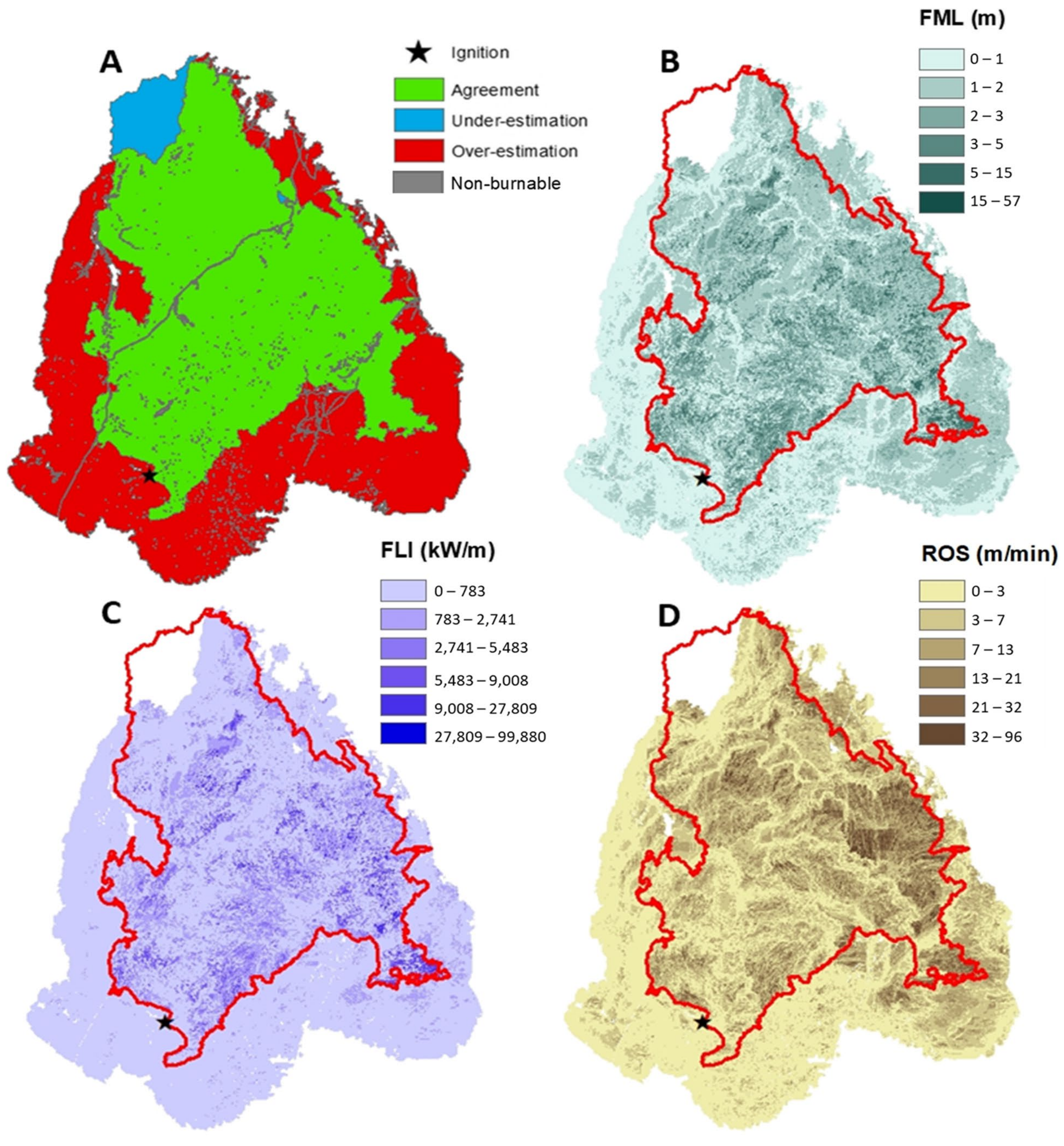

Fig. 4 Maps of FARSITE simulated fire spread and behavior using combination #11's spatial arrangement of fire behavior fuel models as mapped in Fig. 3. **A** Agreement between simulated and observed fire spread where the sum of the blue and green colored polygons is the actual observed burn area, and the sum of green and red polygons is the area burned in FARSITE simulations, **B** simulated flame lengths (FML), **C** simulated fire line intensity (FLI), and **D** simulated rates of fire spread (ROS)

fuel models, after GR4, GR2, GS2, and SH5 were the most frequent (Table 2). GS3 and GR1 contributed to two fuel model combinations, and GR3 and SH7 contributed to one fuel model combination. Fuel model combination #13 had the highest agreement in MTT (SC=0.64, K=0.62) and combination #11 had the highest agreement overall in FARSITE (SC=0.7, K=0.68; Table 2; Figs. 3 and 4). Combination #11 produced 192,000 ha of total fire growth

Table 3 Mean flame length, fireline intensity, and rate of spread values (± standard deviation) for the most accurate FARSITE simulation (combination 11 in Table 2, Figure 3), and maximum simulated rate of spread for each fuel model

Fuel model	Associated vegetation types	FML[a] (m)	FLI[b] (kW/m)	ROS[c] (m/min)	ROS[c] max (m/min)
SH5	Grass-shrubland	2.9 ± 1.1	2,951 ± 2,379	10 ± 7.3	79
GS2	Perennial grassland	1.2 ± 0.6	496 ± 679	5 ± 4	65
GR2	Mixed perennial/annual grassland	1.2 ± 0.6	507 ± 836	8 ± 6.4	95
GR4	Exotic-annual grassland	1.7 ± 0.6	970 ± 739	12 ± 8.7	96

[a] Flame length

[b] Fireline intensity

[c] Rate of spread

over the duration of simulation (8/10/2015–8/15/2015) with 106,000 ha in agreement with the observed perimeter (Fig. 4).

Mean flame length (FML) and fire-line intensity (FLI) for fuel-model combination #11 in FARSITE (Table 3; Fig. 4) were simulated to be too intense for suppression using hand tools (≥ 1.2 m, 350 kW/m). The shrub model (SH5) produced FML and FLI that would likely exceed control by dozers or retardant aircraft (≥ 2.4 m, ≥1700 kW/m). Simulated ROS was highest in the GR4 model, averaging 12 m/min and reaching a maximum of 96 m/min, which is consistent with general observations of the wildfire (Fig. 4). SH5, which occurred in three out of the six most accurate fuel-model combinations, was simulated to have mean FML of nearly 3 m, which is an FML less than observed by firefighters (6–9 m) but is nonetheless an FML that confers uncontrollable fire behavior.

The FARSITE simulations of the Cherry Road fire perimeter, parameterized with FBFMs cross walked from combination #11 from the Soda fire simulations for each respective RAP-based land-cover types (Table 4), had relatively high agreement between simulated and observed burned perimeters with SC and K values ranging from 0.77 to 0.80 and 0.73 to 0.79, respectively (Table 2, Figs. 5 and 6). Another FBFM, GR3, was tested to represent the 4–8% greater annual herbaceous cover indicated by RAP in the mixed perennial and annual grassland cover-type for the Cherry Road (Table 4) compared to the Soda Fire (Table 1). The addition of GR3 slightly improved agreement of simulated to actual fire perimeters, compared to simulations without it. With the addition of GR3, 19,060 ha was simulated to have burned over the entire duration of the simulation (8/21/2016 @ 1300 -> 8/22/2016 @ 1000) with 12,621 ha in agreement with the observed perimeter (Fig. 6).

Discussion

Most applications of MTT and FARSITE use the FBFM maps in LANDFIRE for fuel and canopy inputs, but use of pre-mapped FBFMs from LANDFIRE led to large errors in simulations of the 2015 Soda wildfire. These errors were overcome by informing the selection and spatial arrangement of FBFMs with satellite-derived vegetation cover data. Similar results were noted by Krasnow et al. (2009) who found that simulated-to-observed burned area agreement for two forests fires that burned in Colorado, USA, increased from 77.7 to 91.4% and from 40.3 to 88.2% when utilizing local fuels maps in place of LANDFIRE FBFM maps. Additionally, Massada et al. (2009) noted discrepancies in LANDFIRE maps of non-burnable elements which greatly affected their simulations of fire spread in the wildland urban interface in northern hardwoods of Wisconsin, USA. Though LANDFIRE is one of the best and most available fuels datasets for national level fire analyses in North America, its application may be best suited to large spatial scales owing to reduced accuracy at smaller scales (Scott 2008), and thus, methods for assessment and local tuning of fuel representations are needed. The method of FBFM mapping and assessment we used

Table 4 Land-cover types and their respective fuel models assignments used in Cherry Road FARSITE simulations. Assignments were cross walked from the top performing FARSITE simulations for the Soda wildfire, and GR3 was added because of the greater annual grass cover in the mixed perennial/annual grasslands in the Cherry Road pre-fire data

Land-cover type	Shrub cover (%)	Perennial grass cover (%)	Annual herbaceous cover (%)	Bare soil cover (%)	Assigned fuel models
Perennial grassland	19 ± 6	45 ± 10.9	21 ± 7	15 ± 5.8	GS2
Mixed perennial/annual grassland	9 ±4.2	35 ± 7.4	47 ± 6.2	10 ± 2.8	GR2, GR3
Exotic annual grassland	4 ±2.1	21 ± 5.7	69 ± 8.4	6 ± 2.1	GR4

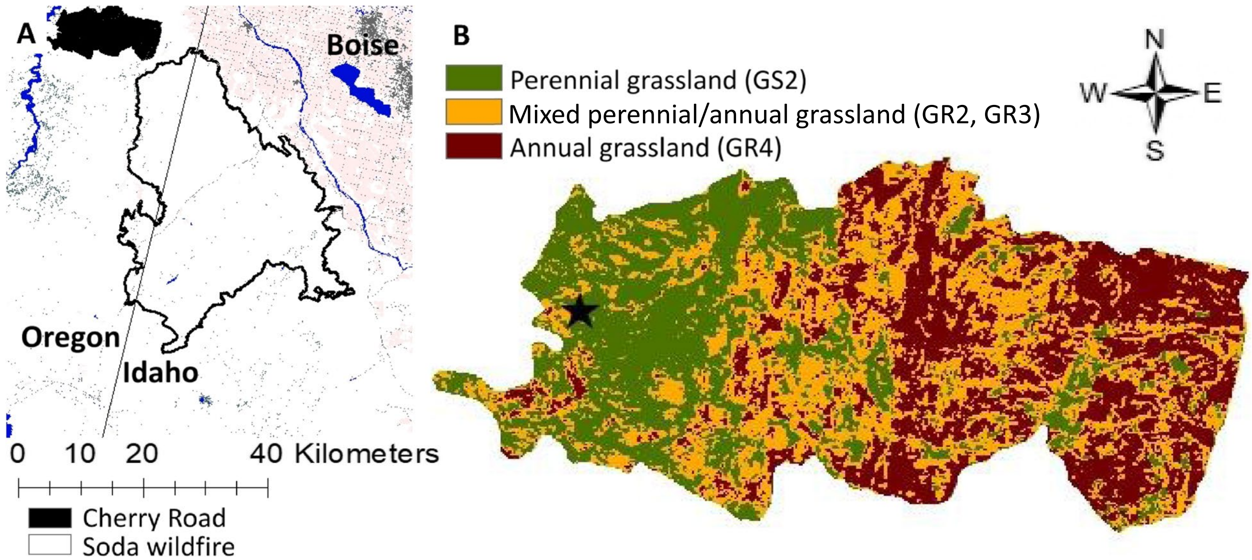

Fig. 5 **A** The 2016 Cherry Road wildfire in relation to the 2015 Soda wildfire. **B** Distribution of land-cover types and corresponding arrays of possible fire behavior fuel models for FARSITE simulations. Land-cover types for the Cherry Road wildfire were generated using the same methods as described for the Soda wildfire. The scale bar aligns to the locator map (panel **A**)

greatly improved agreement between simulated and observed perimeters for the Soda fire. Moreover, cross walking the most accurate fuel-bed parameterization from the Soda fire (combination #11) to the nearby Cherry Road fire also led to relatively high accuracy in FARSITE simulations of the area burned. This model transferability suggests some degree of regional generalizability in the optimal selection of standard FBFMs identified for the Soda Wildfire.

While the optimal fire-spread simulation we identified had relatively high accuracy, it is nonetheless useful to consider possible sources of over- or under-estimation of the area burned. Multiple factors can cause a fire to redirect or extinguish, and thus multiple factors explain the resulting fire boundary, e.g., fire suppression, short-term weather deviations, or non-burnable elements such as roads. Omitting these factors in model simulations of fire spread can detract from simulation accuracy. We sought to mitigate these uncertainties in factors affecting fire boundaries by selectively performing our simulations only in periods when the fires were actively burning and uncontained. For example, we simulated only the first six of 13 total fire days when the Soda fire spread rapidly through a nearly roadless area of dry rangeland fuels and crossed over or around major highways. Similarly, we simulated only the first 21 h of 4 days when the Cherry Road fire actively grew overnight to >90% of its total burned area. Thus, fuels and hourly weather, which were the main factors our modeling considered, were likely the main factors affecting the observed spatial and temporal pattern of burn perimeters and not factors such as fire suppression.

The various disagreements between FARSITE simulations and observed fire perimeters (i.e., Table 2) were due to overestimation of flanking and backfires (Fig. 4). Overpredictions were expected, given the model Rothermel (1972) model assumptions of fuel homogeneity and continuity within pixels. Lateral heterogeneity in actual fuels, i.e., bare-soil canopy gaps between perennial shrubs or grasses which slow or inhibit fire spread, cannot be represented by averages of plant/fuel height and loading that parameterize each pixel for analysis in the models. The excessive flanking and backfires in simulations may also be partially attributable to the coarse 30-m pixel resolution of the model simulations. Whether parameterizing FBFMs at finer spatial scales would further improve the accuracy of MTT and FARSITE simulations could be determined with further research. The lateral and vertical heterogeneity in fuels of sagebrush steppe may require 3-dimensional modeling and consideration of fire-atmospheric interactions such as the feedback that occurs between the fire and local wind flow.

Physics-based fire spread models may offer a means to better account for the effects of lateral heterogeneity in landscapes like sagebrush steppe. Physical models can be parametrized with realistic 3-dimensional vegetation and fuel structure information at resolutions as low as a meter and account for fire-atmosphere feedbacks (Linn et al. 2020). Physical models are still in

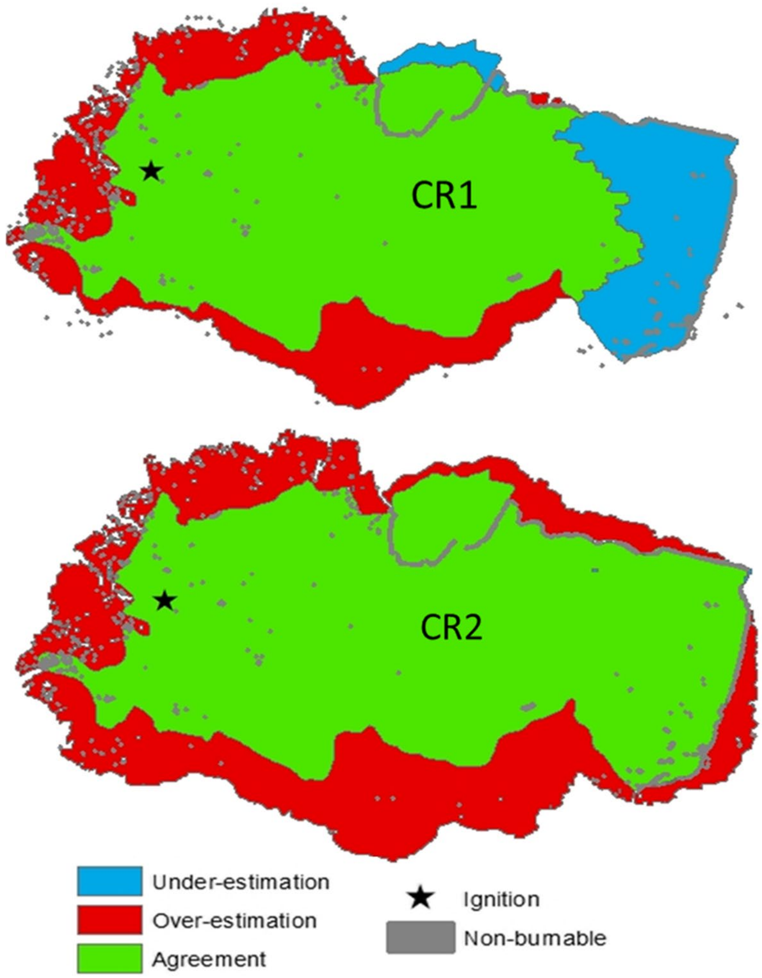

Fig. 6 Agreement between FARSITE simulated spread and the observed burn area for two fire behavior fuel model (FBFM) combinations used for the Cherry Road (CR) fire. FBFMs used in both simulations were GS2 for perennial grasslands, GR4 for annual grasslands. For the mixed perennial-annual grasslands land-cover type, GR2 was used in scenario "CR1" and GR3 was used in "CR2"

development, however, and their complex functionality and intensive data requirements are technical hurdles to their operability. Advances in vegetation and fuels mapping with remote sensing and lidar (Hudak et al. 2020) combined with improved information on past wildfires (Welty and Jeffries 2020) will improve fire-spread modeling applications.

Conclusion

Fire-spread models backed by accuracy assessments help in understanding fire behavior and risks, support active fire suppression, and aid in the design of fuels treatments such as fuel breaks (Finney 2006, Shinneman et al. 2019). Generalized maps of fuel beds, such as from LANDFIRE, may produce simulated fire-spread that differs considerably from observed patterns, as we demonstrated for the Soda Wildfire, and use of LANDFIRE FBFM maps is best preceded by assessment and/or validation prior to application. The model-accuracy assessment and alternative method for FBFM selection we describe are useful advances beyond the field-vegetation map-based accuracy assessments of MTT and FARSITE developed for other semiarid settings, e.g., shrublands of the Mediterranean or Iranian grasslands (Arca et al. 2007; Jahdi et al. 2015, 2016; Salis et al. 2016, 2021). The analysis conducted here may not be feasible for most site-specific applications. However, replicating the FBFM-selection process described here on representative historic burned areas could improve readiness of local or regional fire programs for future, time-sensitive fire applications in their domain.

Supplementary Information

The online version contains supplementary material available at https://doi.org/10.1186/s42408-022-00147-2.

Additional file 1: Supplementary Figure 1. Workflow of steps used in this study. Dashed lines and text color separate data sources/case studiesand shapes differentiate processes and state variables.

Acknowledgements
Kevin Moriarty (BLM) reviewed the manuscript and provided helpful comments, Mark Finney of the USFS provided initial consultation, and Michelle Crist of the BLM provided project support. Any use of trade, firm, or product names is for descriptive purposes only and does not imply endorsement by the US Government.

Authors' contributions
MJG conceived of, supervised, and procured the funding of the project. SJP performed the analyses. Both authors wrote, edited, read, and approved the final manuscript.

Funding
Funding was provided by the Bureau of Land Management.

Availability of data and materials
The datasets used for this study can be obtained directly from MTBS (mtbs.gov), LANDFIRE (landfire.gov), and RAP (rangelands.app).

Declarations

Ethics approval and consent to participate
Not applicable.

Consent for publication
Not applicable.

Competing interests
The authors declare that they have no competing interests.

Received: 20 November 2021 Accepted: 30 August 2022
Published online: 24 September 2022

References

Albini, F.A. 1976. *Estimating wildfire behavior and effects (Vol. 30).* Department of Agriculture, Forest Service, Intermountain Forest and Range Experiment Station.
Alexander, M.E., and M.G. Cruz. 2013. Are the applications of wildland fire behaviour models getting ahead of their evaluation again? *Environmental Modelling Software* 41: 65–71.
Allred, B.W., B.T. Bestelmeyer, C.S. Boyd, C. Brown, K.W. Davies, M.C. Duniway, L.M. Ellsworth, T.A. Erickson, S.D. Fuhlendorf, T.V. Griffiths, and V. Jansen. 2021. Improving Landsat predictions of rangeland fractional cover with multitask learning and uncertainty. *Methods in Ecology and Evolution* 12 (5): 841–849.
Anderson, D.H., E.A. Catchpole, N.J. De Mestre, and T. Parkes. 1982. Modelling the spread of grass fires. *The ANZIAM Journal* 23 (4): 451–466.
Anderson, H.E. 1982. *Aids to determining fuel models for estimating fire behavior (Vol. 122).* US Department of Agriculture, Forest Service, Intermountain Forest and Range Experiment Station.
Applestein, C., and M.J. Germino. 2021. Detecting shrub recovery in sagebrush steppe: Comparing Landsat-derived maps with field data on historical wildfires. *Fire Ecology* 17 (1): 1–11.
Applestein, C., and M.J. Germino. 2022. How do accuracy and model agreement vary with versioning, scale, and landscape heterogeneity for satellite-derived vegetation maps in sagebrush steppe? *Ecological Indicators* 139: 108935.
Arca, B., P. Duce, M. Laconi, G. Pellizzaro, M. Salis, and D. Spano. 2007. Evaluation of FARSITE simulator in Mediterranean maquis. *International Journal Wildland of Fire* 16 (5): 563–572.
Balch, J.K., B.A. Bradley, C.M. D'Antonio, and J. Gómez-Dans. 2013. Introduced annual grass increases regional fire activity across the arid western USA (1980–2009). *Global Change Biology* 19 (1): 173–183.
Davidson, B.E., M.J. Germino, B. Richardson, and D.M. Barnard. 2019. Landscape and organismal factors affecting sagebrush-seedling transplant survival after megafire restoration. *Restoration Ecology* 27 (5): 1008–1020.
Dennison, P.E., S.C. Brewer, J.D. Arnold, and M.A. Moritz. 2014. Large wildfire trends in the western United States, 1984–2011. *Geophysical Research Letters* 41 (8): 2928–2933.
Filippi, J.B., V. Mallet, and B. Nader. 2014. Evaluation of forest fire models on a large observation database. *Natural Hazards Earth System Sciences* 14 (11): 3077–3091.
Finney, M.A. 2002. Fire growth using minimum travel time methods. *Canadian Journal of Forest Research* 32 (8): 1420–1424.
Finney, M.A. 1998. *FARSITE, Fire Area Simulator--model development and evaluation* (No. 4). US Department of Agriculture, Forest Service, Rocky Mountain Research Station.
Finney, M.A. 2006. An overview of FlamMap fire modeling capabilities. In *Fuels Management-How to Measure Success: Conference Proceedings. 28-30 March 2006; Portland, OR. Proceedings RMRS-P-41*, ed. Patricia L. Andrews, Bret W. Butler, comps. 2006, 213–220. Fort Collins, CO: US Department of Agriculture, Forest Service, Rocky Mountain Research Station (Vol. 41).
Germino, M.J., D.M. Barnard, B.E. Davidson, R.S. Arkle, D.S. Pilliod, M.R. Fisk, and C. Applestein. 2018. Thresholds and hotspots for shrub restoration following a heterogeneous megafire. *Landscape Ecology* 33 (7): 1177–1194.
Germino, M.J., P. Torma, M.R. Fisk, and C.V. Applestein. 2022. Monitoring for adaptive management of burned sagebrush-steppe rangelands: addressing variability and uncertainty on the 2015 Soda Megafire. *Rangelands* 44 (1): 99–110.
Germino, M.J., J. Belnap, J.M. Stark, E.B. Allen, and B.M. Rau. 2016. Ecosystem impacts of exotic annual invaders in the genus Bromus. In *Exotic bromegrasses in arid and semiarid ecosystems of the Western US*, 61–95. Cham: Springer.
Hudak, A.T., A. Kato, B.C. Bright, E.L. Loudermilk, C. Hawley, J.C. Restaino, R.D. Ottmar, G.A. Prata, C. Cabo, S.J. Prichard, and E.M. Rowell. 2020. Towards spatially explicit quantification of pre-and postfire fuels and fuel consumption from traditional and point cloud measurements. *Forest Science* 66 (4): 428–442.
Jahdi, R., M. Salis, A.A. Darvishsefat, M.A. Mostafavi, F. Alcasena, V. Etemad, O. Lozano, and D. Spano. 2015. Calibration of FARSITE simulator in northern Iranian forests. *Natural Hazards and Earth System Science* 15 (3): 443–459.
Jahdi, R., M. Salis, A.A. Darvishsefat, F. Alcasena, M.A. Mostafavi, V. Etemad, O.M. Lozano, and D. Spano. 2016. Evaluating fire modelling systems in recent wildfires of the Golestan National Park, Iran. *Forestry* 89 (2): 136–149.
Jewell, S. 2015. *Department of the Interior Secretarial Order No. 3336. Rangeland Fire Prevention, Management and Restoration*, 4.
Jones, M.O., B.W. Allred, D.E. Naugle, J.D. Maestas, P. Donnelly, L.J. Metz, J. Karl, R. Smith, B. Bestelmeyer, C. Boyd, and J.D. Kerby. 2018. Innovation in rangeland monitoring: annual, 30 m, plant functional type percent cover maps for US rangelands, 1984–2017. *Ecosphere* 9 (9): 02430.
Krasnow, K., T. Schoennagel, and T.T. Veblen. 2009. Forest fuel mapping and evaluation of LANDFIRE fuel maps in Boulder County, Colorado, USA. *Forest Ecology Manag* 257 (7): 1603–1612.
Linn, R.R., S.L. Goodrick, S. Brambilla, M.J. Brown, R.S. Middleton, J.J. O'Brien, and J.K. Hiers. 2020. QUIC-fire: A fast-running simulation tool for prescribed fire planning. *Environmental Modelling Software* 125: 104616.
Massada, A.B., V.C. Radeloff, S.I. Stewart, and T.J. Hawbaker. 2009. Wildfire risk in the wildland–urban interface: A simulation study in northwestern Wisconsin. *Forest Ecology Management* 258 (9): 1990–1999.
Noonan-Wright, E.K., T.S. Opperman, M.A. Finney, G.T. Zimmerman, R.C. Seli, L.M. Elenz, D.E. Calkin, and J.R. Fiedler. 2011. Developing the US wildland fire decision support system. *Journal of Combustion.* 168473: 14.
NOAA NIDIS, National Oceanic and Atmospheric Administration, National Integrated Drought Information System. *Drought Conditions for Owyhee County*. Available at: https://www.drought.gov/states/idaho/county/owyhee. Accessed June 2021
Richards, G.D. 1995. A general mathematical framework for modeling two-dimensional wildland fire spread. *International Journal of Wildland Fire* 5 (2): 63–72.

Rothermel, R.C. 1972. *A mathematical model for predicting fire spread in wildland fuels (Vol. 115)* Intermountain Forest & Range Experiment Station, Forest Service, US Department of Agriculture.
Salis, M., B. Arca, F. Alcasena, M. Arianoutsou, V. Bacciu, P. Duce, B. Duguy, N. Koutsias, G. Mallinis, I. Mitsopoulos, and J.M. Moreno. 2016. Predicting wildfire spread and behaviour in Mediterranean landscapes. *International Journal of Wildland Fire* 25 (10): 1015–1032.
Salis, M., B. Arca, L. Del Giudice, P. Palaiologou, F. Alcasena-Urdiroz, A. Ager, M. Fiori, G. Pellizzaro, C. Scarpa, M. Schirru, and A. Ventura. 2021. Application of simulation modeling for wildfire exposure and transmission assessment in Sardinia, Italy. *International Journal of Disaster Risk Reduction* 58: 102189.
Scott, J.H., and R.E. Burgan. 2005. *Standard fire behavior fuel models: A comprehensive set for use with Rothermel's surface fire spread model. Gen. Tech. Rep. RMRS-GTR-153*. Fort Collins, CO: Department of Agriculture, Forest Service, Rocky Mountain Research Station.
Scott, J.H. 2008. *Review and assessment of LANDFIRE canopy fuel mapping procedures* LANDFIRE Bulletin: US Department of Agriculture, Fort Collins USA.
Shinneman, D.J., M.J. Germino, D.S. Pilliod, C.L. Aldridge, N.M. Vaillant, and P.S. Coates. 2019. The ecological uncertainty of wildfire fuel breaks: Examples from the sagebrush steppe. *Frontiers Ecology Environment* 17 (5): 279–288.
Soda Fire Fuel Breaks Project Environmental Impact Statement. 2017. Available at: https://eplanning.blm.gov/public_projects/nepa/58797/99136/120154/DOI-BLM-ID-B030-2016-0003-EA-Final.pdf. Accessed May 2021.
Stratton, R.D. 2009. *Guidebook on LANDFIRE fuels data acquisition, critique, modification, maintenance, and model calibration (No. 220)* US Department of Agriculture, Forest Service, Rocky Mountain Research Station.
National Fuel Moisture Database. United States Forest Service, Wildland Fire Assessment System. Available at: https://www.wfas.net/index.php/national-fuel-moisture-database-moisture-drought-103. Accessed June 2021.
Welty, J.L., and M.I. Jeffries. 2020. *Combined wildfire datasets for the United States and certain territories, 1878-2019: U.S. Geological Survey data release.* https://doi.org/10.5066/P9Z2VVRT. Accessed June 2021.
WFDSS: United States Geologic Survey, Wildland fire Decision Support System. Available at: https://wfdss.usgs.gov/wfdss/WFDSS_Contactus.shtml. Accessed Nov 2021.

Publisher's Note